

# Synthesis and Electrochemical Behavior of a Zwitterion-Bridged Metalla-Cage

Minghui Yuan,<sup>†,‡</sup> Fritz Weisser,<sup>§</sup> Biprajit Sarkar,<sup>§</sup> Amine Garci,<sup>†</sup> Pierre Braunstein,<sup>\*,‡</sup> Lucie Routaboul,<sup>\*,‡</sup> and Bruno Therrien<sup>\*,†</sup>

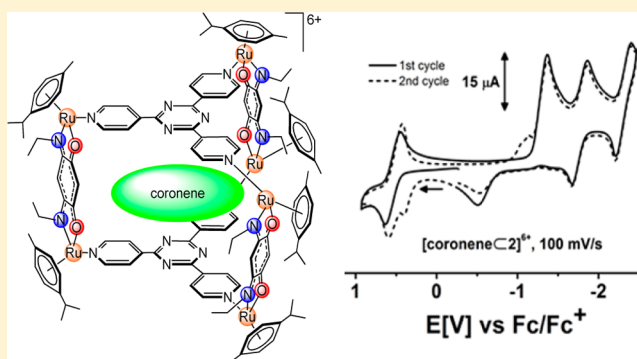
<sup>†</sup>Institut de Chimie, Université de Neuchâtel, 51 Avenue de Bellevaux, CH-2000 Neuchâtel, Switzerland

<sup>‡</sup>Laboratoire de Chimie de Coordination, Institut de Chimie (UMR 7177 CNRS), Université de Strasbourg, 4 rue Blaise Pascal, F-67081 Strasbourg Cédex, France

<sup>§</sup>Institut für Chemie und Biochemie, Freie Universität Berlin, Fabeckstraße 34-36, D-14195 Berlin, Germany

## Supporting Information

**ABSTRACT:** The electrochemical behavior of a dinuclear arene ruthenium complex containing a zwitterionic bridging ligand and of a hexacationic metalla-prism obtained from the assembly of three dinuclear zwitterion-bridged units and two tridentate panels has been investigated. The encapsulation of coronene in the hydrophobic cavity of the metalla-prism stabilizes the assembly and subsequently modifies the redox potentials of the hexanuclear metalla-prism.

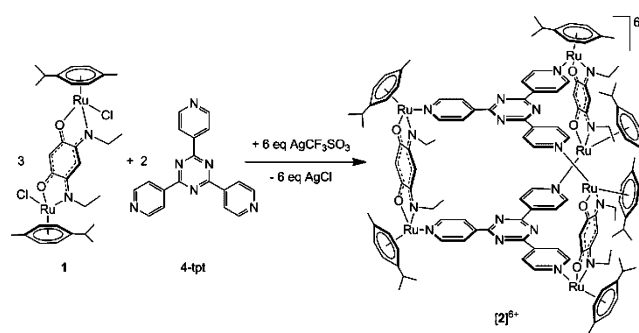


The coordination-driven strategy to generate metalla-assemblies is now well established. Initially dominated by square-planar metal centers,<sup>1</sup> nowadays tetrahedral and octahedral metal centers are also extensively used.<sup>2</sup> The shift from square-planar (four coordination sites) to octahedral geometry (six coordination sites) and the utilization of other metal centers have allowed the introduction of new ligands, thus increasing the functionality potential of metalla-assemblies. Among these ligands, zwitterionic quinonoid ligands are particularly attractive.<sup>3</sup> The redox activity of zwitterion ligands is quite remarkable, due to the electronic nature of these molecules.<sup>4</sup> Herein, we present the first dinuclear arene ruthenium complex bridged by a zwitterionic quinonoid ligand, (*p*-cymene)<sub>2</sub>Ru<sub>2</sub>Cl<sub>2</sub>L (**1**; LH<sub>2</sub> = (6Z)-4-(ethylamino)-6-(ethylimino)-3-oxocyclohexa-1,4-dien-1-olate). Furthermore, this neutral dinuclear complex forms in the presence of silver triflate and 2,4,6-tris(pyridin-4-yl)-1,3,5-triazine (4-tpt) a cationic metalla-prism of the general formula [(*p*-cymene)<sub>6</sub>Ru<sub>6</sub>L<sub>3</sub>(4-tpt)<sub>2</sub>](CF<sub>3</sub>SO<sub>3</sub>)<sub>6</sub> ([**2**](CF<sub>3</sub>SO<sub>3</sub>)<sub>6</sub>) (see Scheme 1).

Metalla-prism [**2**]<sup>6+</sup> possesses a cavity large enough to accommodate guest molecules, and upon addition of coronene during the formation of metalla-prism [**2**](CF<sub>3</sub>SO<sub>3</sub>)<sub>6</sub> from **1** and 4-tpt, the filled metalla-prism [coroneneC**2**](CF<sub>3</sub>SO<sub>3</sub>)<sub>6</sub> is obtained in very good yield (75%) (see Scheme 2).

The formation of metalla-prism [**2**]<sup>6+</sup> and the carceplex system [coroneneC**2**]<sup>6+</sup> can easily be monitored by <sup>1</sup>H NMR spectroscopy. In [**2**]<sup>6+</sup>, the four diastereotopic aromatic protons of the *p*-cymene ligands are shifted downfield by ~0.4 ppm in

**Scheme 1. Synthesis of Metalla-Prism [**2**]<sup>6+</sup> from **1** and 4-tpt in the Presence of AgCF<sub>3</sub>SO<sub>3</sub>**



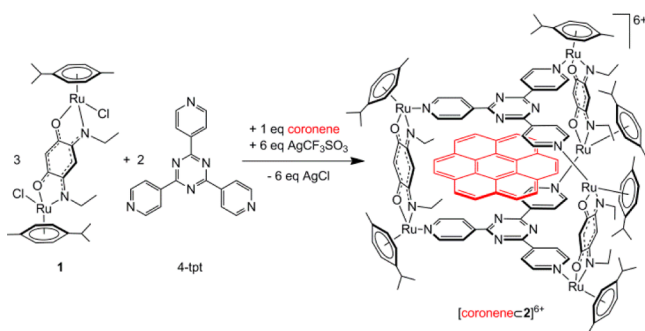
comparison to those of **1** (Figures S1 and S2, Supporting Information). However, the C–H protons of the bridging zwitterionic ligand ( $\delta$  5.77 and 5.01 ppm) are slightly shifted upfield by 0.04 ppm upon formation of [**2**]<sup>6+</sup>, while the same C–H protons are strongly shifted downfield ( $\delta$  6.39 and 5.61 ppm) when coronene is trapped in the cavity (Figure S3, Supporting Information). The encapsulation of coronene in the cavity of [**2**]<sup>6+</sup> is further confirmed by diffusion-ordered NMR spectroscopy (DOSY). Indeed, the singlet associated with

**Special Issue:** Organometallic Electrochemistry

**Received:** February 12, 2014

**Published:** May 12, 2014

**Scheme 2. Synthesis of [coroneneC2]<sup>6+</sup> from 1, 4-tpt, and Coronene in the Presence of AgCF<sub>3</sub>SO<sub>3</sub>**

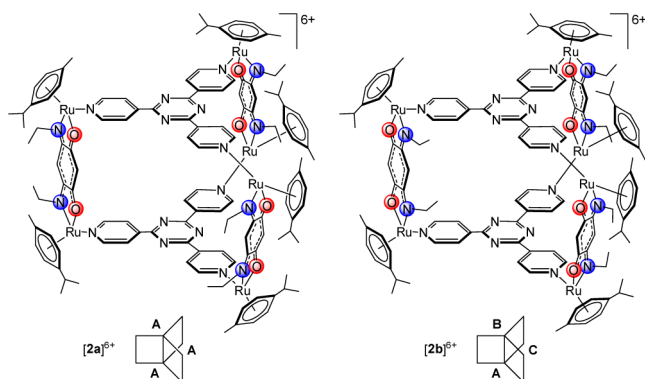


coronene clearly diffuses with the signals associated with the metalla-cage (Figure S4, Supporting Information), thus corroborating the entrapment of coronene in the hydrophobic cavity of [2]<sup>6+</sup>. Electrospray ionization mass spectrometry also supports the suggested structures of 1, [2](CF<sub>3</sub>SO<sub>3</sub>)<sub>6</sub>, and [coroneneC2](CF<sub>3</sub>SO<sub>3</sub>)<sub>6</sub> (Figures S5–S7, Supporting Information). A peak corresponding to [1 – Cl]<sup>+</sup> at *m/z* 699.1 is observed for 1, while for the metalla-prism [2]<sup>6+</sup>, the peak corresponding to the intact metalla-prism [2 + 4 CF<sub>3</sub>SO<sub>3</sub>]<sup>2+</sup> is observed at *m/z* 1605.2. Similarly, the peak corresponding to [2 + coronene + 4 CF<sub>3</sub>SO<sub>3</sub>]<sup>2+</sup> at *m/z* 1754.7 is observed in the ESI-MS spectrum of [coroneneC2](CF<sub>3</sub>SO<sub>3</sub>)<sub>6</sub>. Peaks associated with fragments of the metalla-cages are also observed in the ESI-MS spectra of [2](CF<sub>3</sub>SO<sub>3</sub>)<sub>6</sub> and [coroneneC2]-(CF<sub>3</sub>SO<sub>3</sub>)<sub>6</sub>.

The presence of three zwitterionic bridges in the metalla-prism [2]<sup>6+</sup> can potentially give rise to two isomers. The first is a symmetrical isomer [2a]<sup>6+</sup> in which the *N,N'*-diethyl edge of the zwitterionic ligands always faces the *O,O'* edge of the neighboring zwitterionic bridging unit, while in the unsymmetrical isomer [2b]<sup>6+</sup>, two *N,N'*-diethyl edges are facing each other and the remaining *N,N'*-diethyl edge is facing an *O,O'* edge, thus generating an unsymmetrical metalla-prism with three nonequivalent segments (Scheme 3). Although the presence of these two isomers (2a,b) is suggested by the broadness of several <sup>1</sup>H NMR signals, it could not be unambiguously confirmed.

Preliminary electrochemical investigations were carried out on the dinuclear complex 1 and the metalla-prisms [2]<sup>6+</sup> and

**Scheme 3. Schematic Representations of the Symmetrical Isomer [2a]<sup>6+</sup> (Left) and the Unsymmetrical Isomer [2b]<sup>6+</sup> (Right) Including the Identification of Their Respective Trigonal Segments**



[coroneneC2]<sup>6+</sup>. Complex 1 displays an oxidation step at 0.27 V and a reduction step at –1.83 V, both of which are irreversible on the electrochemical time scale (Figure 1). A

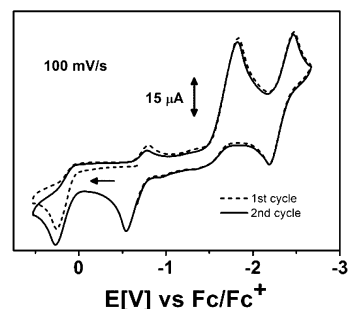


**Figure 1.** Cyclic voltammogram of 1 in THF/0.1 M Bu<sub>4</sub>NPF<sub>6</sub> at 298 K.

further quasi-reversible reduction step is observed at –2.33 V. The current height of the rereduction peak associated with the first oxidation increases at faster scan rates (Figure S8, Supporting Information) and at lower temperatures (Figure S9, Supporting Information). A further rereduction peak associated with the first oxidation step is observed at –0.8 V. The first reduction peak remains electrochemically irreversible even at faster scan rates, and a shifted reoxidation peak is observed at –0.5 V (Figure 1 and Figure S10 (Supporting Information)). For the quasi-reversible second reduction step at –2.33 V, the peak currents for the anodic and cathodic waves are similar, but the separation between the two waves is large and increases with increasing scan rates (Figure 1 and Figure S11 (Supporting Information)). Using a modified Baranski method,<sup>5</sup> the numbers of electrons transferred were estimated, using the two different standards ferrocene and *p*-benzoquinone, to be 1 for the oxidation step, 3 for the first reduction step, and 2 for the second reduction step. UV–vis–NIR spectroelectrochemistry was used to monitor the chemical reversibility of the redox steps. These results showed the first oxidation as well as the first and the second reduction steps to be chemically reversible, as judged by the regeneration of the initial UV–vis–NIR spectrum of 1 to about 90% on scanning the potential back (Figures S12 and S13, Supporting Information). The spectroelectrochemical results thus point to an EC (electron transfer, chemical reaction) or a more complex mechanism.

The metalla-prisms [2]<sup>6+</sup> and [coroneneC2]<sup>6+</sup> display redox responses that have strong similarities to those of 1 (Figure 2), albeit with potentials that are positively shifted in comparison to those of 1 (Table S1, Supporting Information). This can be

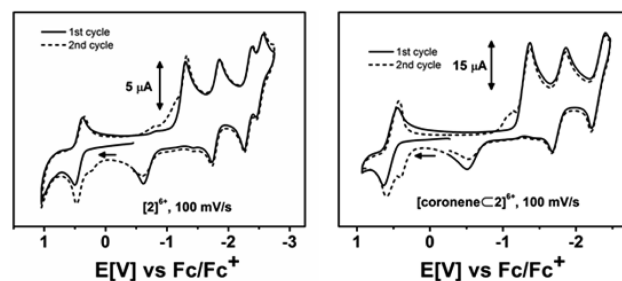


**Figure 2.** Cyclic voltammograms of [2]<sup>6+</sup> and [coroneneC2]<sup>6+</sup> in THF/0.1 M Bu<sub>4</sub>NPF<sub>6</sub> at 298 K.

explained by the  $\pi$ -accepting nature of the 4-tpt ligand present in the metalla-prisms. Additionally, metalla-prisms  $[2]^{6+}$  and  $[\text{coroneneC}2]^{6+}$  show two further reduction waves at higher negative potentials (Figure 2). The differences in potentials between the oxidation and the first and second reduction peaks are similar in **1**,  $[2]^{6+}$ , and  $[\text{coroneneC}2]^{6+}$ . These data strongly point to the oxidation and the first two reduction processes in  $[2]^{6+}$  and  $[\text{coroneneC}2]^{6+}$  taking place within the  $\{\text{Ru}(\text{L}^{2-})\text{Ru}\}$  units. The third and the fourth reduction steps are likely 4-tpt based. For  $[2]^{6+}$  and  $[\text{coroneneC}2]^{6+}$  the numbers of electrons transferred are 3 for the oxidation, 9 for the first reduction, and 6 for the second reduction. The oxidation step for the metalla-prisms is electrochemically more reversible than for **1**. However, for  $[2]^{6+}$  the currents of both the forward and back processes decrease after several cycles, whereas for  $[\text{coroneneC}2]^{6+}$  they remain stable. Thus, the guest molecule is seen to impart additional stability to the prism and makes it more stable toward redox reactions.

In conclusion, we have presented here the synthesis and characterization of the dinuclear complex **1**, the first example of the corresponding metalla-prism  $[2]^{6+}$ , and the carceplex system  $[\text{coroneneC}2]^{6+}$ , all with zwitterionic redox-active ligands. Preliminary electrochemical investigations reveal the potential of the metalla-prisms to act as multielectron reservoirs and the ability of guest molecules to provide redox stability to the metalla-prisms. Even though the Baranski method has been used for determining the electron count in these systems, this method has certain limitations for complicated redox systems. Future work will focus in dealing with this issue. Details of the spectroscopic signatures of the various redox states, their corresponding electronic structures, and the involved redox mechanisms will be reported in the near future.

## ■ ASSOCIATED CONTENT

### ■ Supporting Information

General remarks and details of the synthesis of **1**, metalla-prism  $[2](\text{CF}_3\text{SO}_3)_6$ , and  $[\text{coroneneC}2](\text{CF}_3\text{SO}_3)_6$  along with their corresponding  $^1\text{H}$  NMR, DOSY, and ESI mass spectra, cyclic voltammograms, electrochemical potentials, and UV-vis-NIR spectra. This material is available free of charge via the Internet at <http://pubs.acs.org>.

## ■ AUTHOR INFORMATION

### Corresponding Authors

\*E-mail for P.B.: [braunstein@unistra.fr](mailto:braunstein@unistra.fr).

\*E-mail for L.R.: [lroutaboul@unistra.fr](mailto:lroutaboul@unistra.fr).

\*E-mail for B.T.: [bruno.therrien@unine.ch](mailto:bruno.therrien@unine.ch).

### Author Contributions

The manuscript was written through contributions of all authors, and all authors have given approval to the final version of this manuscript.

### Notes

The authors declare no competing financial interest.

## ■ ACKNOWLEDGMENTS

This paper is dedicated to Prof. Barry Lever (Toronto) for his outstanding contributions to chemistry, and coordination chemistry in particular. We are grateful to the CNRS (L.R. and P.B.), the Ministère de la Recherche (Paris), the Université de Strasbourg and the Région Alsace (Ph.D. grant to M.Y.) for financial support. The Fonds der Chemischen Industrie (FCI) is kindly acknowledged (F.W. and B.S.) for the financial

support of this project. Financial support of this work by the Swiss National Science Foundation (A.G.) and the University of Neuchâtel (M.Y.) and a generous loan of ruthenium(III) chloride hydrate from the Johnson Matthey Research Centre are gratefully acknowledged.

## ■ REFERENCES

- (1) (a) Fujita, M. *Acc. Chem. Res.* **1999**, *32*, 53–61. (b) Leininger, S.; Olenyuk, B.; Stang, P. J. *Chem. Rev.* **2000**, *100*, 853–908. (c) Fujita, M.; Tominaga, M.; Hori, A.; Therrien, B. *Acc. Chem. Res.* **2005**, *38*, 371–380. (d) You, C.-C.; Hippus, C.; Gruene, M.; Wuerthner, F. *Chem. Eur. J.* **2006**, *12*, 7510–7519. (e) Northrop, B. H.; Gloeckner, A.; Stang, P. J. *J. Org. Chem.* **2008**, *73*, 1787–1794. (f) Chakrabarty, R.; Mukherjee, P. S.; Stang, P. J. *Chem. Rev.* **2011**, *111*, 6810–6918. (g) Vajpayee, V.; Kim, H.; Mishra, A.; Mukherjee, P. S.; Stang, P. J.; Lee, M. H.; Kim, H. K.; Chi, K.-W. *Dalton Trans.* **2011**, *40*, 3112–3115. (h) Vajpayee, V.; Song, Y. H.; Jung, Y. J.; Kang, S. C.; Kim, H.; Kim, I. S.; Wang, M.; Cook, T. R.; Stang, P. J.; Chi, K.-W. *Dalton Trans.* **2012**, *41*, 3046–3052.
- (2) (a) Lee, S. J.; Hupp, J. T. *Coord. Chem. Rev.* **2006**, *250*, 1710–1723. (b) Therrien, B. *Eur. J. Inorg. Chem.* **2009**, 2445–2453. (c) Han, Y.-F.; Li, H.; Zheng, Z.-F.; Jin, G.-X. *Chem. Asian J.* **2012**, *7*, 1243–1250. (d) Hall, B. R.; Adams, H.; Ward, M. D. *Supramol. Chem.* **2012**, *24*, 499–507. (e) Ward, M. D.; Raithby, P. R. *Chem. Soc. Rev.* **2013**, *42*, 1619–1636. (f) Smulders, M. M. J.; Riddell, I. A.; Browne, C.; Nitschke, J. R. *Chem. Soc. Rev.* **2013**, *42*, 1728–1754. (g) Singh, A. K.; Pandey, D. S.; Xu, Q.; Braunstein, P. *Coord. Chem. Rev.* **2014**, *270*–271, 31–56.
- (3) (a) Braunstein, P.; Siri, O.; Taquet, J.-P.; Rohmer, M.-M.; Bénard, M.; Welter, R. J. *Am. Chem. Soc.* **2003**, *125*, 12246–12256. (b) Taquet, J.-P.; Siri, O.; Braunstein, P.; Welter, R. *Inorg. Chem.* **2004**, *43*, 6944–6953. (c) Yang, Q.-Z.; Siri, O.; Braunstein, P. *Chem. Eur. J.* **2005**, *11*, 7237–7246. (d) Yang, Q.-Z.; Kermagoret, A.; Agostinho, M.; Siri, O.; Braunstein, P. *Organometallics* **2006**, *25*, 5518–5527. (e) Braunstein, P.; Siri, O.; Steffanut, P.; Winter, M.; Yang, Q.-Z. *C. R. Chim.* **2006**, *9*, 1493–1499. (f) Routaboul, L.; Braunstein, P.; Xiao, J.; Zhang, Z.; Dowben, P. A.; Dalmás, G.; Da Costa, V.; Felix, O.; Decher, G.; Rosa, L. G.; Doudin, B. *J. Am. Chem. Soc.* **2012**, *134*, 8494–8506. (g) Kunkel, D. A.; Simpson, S.; Nitz, J.; Rojas, G. A.; Zurek, E.; Routaboul, L.; Doudin, B.; Braunstein, P.; Dowben, P. A.; Enders, A. *Chem. Commun.* **2012**, *48*, 7143–7145. (h) Simpson, S.; Kunkel, D. A.; Hooper, J.; Nitz, J.; Dowben, P. A.; Routaboul, L.; Braunstein, P.; Doudin, B.; Enders, A.; Zurek, E. *J. Phys. Chem. C* **2013**, *117*, 16406–16415.
- (4) (a) Braunstein, P.; Bubrin, D.; Sarkar, B. *Inorg. Chem.* **2009**, *48*, 2534–2540. (b) Das, H. S.; Das, A. K.; Pattacini, R.; Huebner, R.; Sarkar, B.; Braunstein, P. *Chem. Commun.* **2009**, 4387–4389. (c) Paretzki, A.; Pattacini, R.; Huebner, R.; Braunstein, P.; Sarkar, B. *Chem. Commun.* **2010**, *46*, 1497–1499. (d) Deibel, N.; Schweinfurth, D.; Huebner, R.; Braunstein, P.; Sarkar, B. *Dalton Trans.* **2011**, *40*, 431–436. (e) Hohloch, S.; Braunstein, P.; Sarkar, B. *Eur. J. Inorg. Chem.* **2012**, 546–553. (f) Deibel, N.; Hohloch, S.; Sommer, M. G.; Schweinfurth, D.; Ehret, F.; Braunstein, P.; Sarkar, B. *Organometallics* **2013**, *32*, 7366–7375.
- (5) Baranski, A. S.; Fawcett, W. R.; Gilbert, C. M. *Anal. Chem.* **1985**, *57*, 166–170.